Lab on a Chip

Devices and applications at the micro- and nanoscale

Accepted Manuscript

This article can be cited before page numbers have been issued, to do this please use: N. Yu, Y. Liu, S. Wang, X. Tang, P. Ge, J. Nan, J. Zhang and B. Yang, *Lab Chip*, 2019, DOI: 10.1039/C9LC00730J.

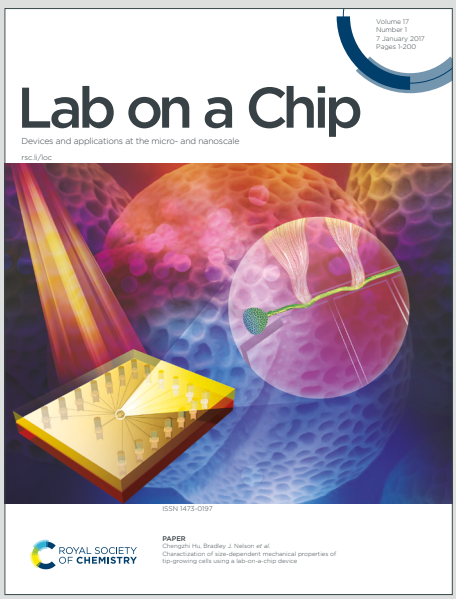

ROYAL SOCIETY OF CHEMISTRY

rsc.li/loc

View Article Online
DOI: 10.1039/C9LC00730J

COMMUNICATION

Pressure-controlled microfluidic sub-picoliter ultramicro-volume syringes based on integrated micro-nanostructure arrays

Received 00th January 20xx,
Accepted 00th January 20xx

DOI: 10.1039/x0xx00000x

Nianzuo Yu,[a] Yongshun Liu,*[,b] Shuli Wang,[c,d] Xiaoduo Tang,[a] Peng Ge,[a] Jingjie Nan,[a] Junhu Zhang,*[,a] and Bai Yang[a]

Ultramicro-volume syringes are fabricated by integrating micro-nanostructure arrays in microchannels for dispensing quantitative sub-picoliter liquids. The minimum of available liquid volume is in increments as low as 0.5 pL with 96% accuracy. Specifically, controllable synthesis of nanocrystals could be produced in a lab-on-chip platform which integrated with the syringes.

Precise manipulation of liquid volume (less than picoliter) is greatly needed in the fields of point-of-care diagnostic technologies,[1-2] drug synthesis,[3-5] cell cultures,[6-8] and even directly drug injection to cells.[9-12] Commercial manipulation methods for liquid volume include the preparation of Echo systems[13-14] and scanning probes,[15-16] but it is still challenging to take into account both the integratability and continuity of dispensing process. In general, the diameter of a 10-pL droplet is near 10 μm, which is matching with microfluidic devices, and the enclosed microchip could prevent the evaporation of liquids.[17-22] Conventional droplet microfluidics show advantages in controlling the size of multiphase droplets in a high-throughput way, but the use of surfactant is necessary for most droplet microfluidics devices, which is inconvenient to extract separate quantitative droplet and execute follow-up processing.[23-25] A recently developed fluidic force microscopy have the potential to inject and extract measurable liquids to single cell for molecular analyses, while expensive assistant equipment may limit the promotion to general laboratory.[26-27]

Owing to lower operating cost and great manipulation ability for fluids, microvalves offer opportunities in regulating the volume of liquids.[28-29] Capillary valve constructed microchip can reduce the order of magnitude of the liquid volume to sub-nanoliter level,[30-31] however, it is hard to further decrease the volume due to the blocking of the PDMS slabs for tens of micrometer microchannels. Furthermore, as for a device which is used for dispensing quantitative liquids, accuracy and repeatability are the crucial characterization parameters, deformable elastic materials and its undefined triple-phase contact line (TCL) for liquids may contribute to measuring errors. Recent advances of rigid Laplace microvalve have demonstrated its accurate manipulation ability for liquid volume.[32-33] However, most of the devices can only obtain a fixed liquid volume, and are not easy to be integrated into other devices. As a result, successive sub-picoliter liquids are not easy to capture, and actual utilization of the liquid to real applications remains challenging.

In this communication, pressure-controlled ultramicro-volume syringes (UVSs) are employed to successively dispense quantitative sub-picoliter liquids. Microstripe array which embedded with numerous nanopillars (MSNP) is adopted as the substrate of UVS. As illustrated in **Scheme 1**, we designed a trapezoid-shaped microfluidic channel, which are separated into a series of chambers with pre-set volume by gradient-length MSNP arrays. The volume of captured liquids and the measuring range of the UVS could be modified by changing the applied pressure of inlets and the dimensions of the microchannel. To prevent the deformation of microchannel and reduce the volume of available liquid, glass-Si constructed UVS (G-UVS) has been fabricated, and obtainable minimum volume of liquid could reach 0.5 pL with 96% accuracy. The UVS also shows great applicability for fluids with wide surface tension (ST) ranges. To demonstrate the practical application of the syringe, a microchip which consists of three UVSs was designed, and gradient-size Au nanoparticles and anisotropic Au nanorods have been successfully synthesized. The UVS provides novel insights into resource-limited diagnosis, synthetic reactions of lab-on-chip applications, measurable cell cultures and quantitative drug transport, which may also contribute to the research of direct injection of drug for single cell.

Results and disscussion

Capture of quantitative liquids by the UVS

[a] State Key Laboratory of Supramolecular Structure and Materials, College of Chemistry, Jilin University, 130012, P. R. China.
[b] State Key Laboratory of Applied Optics, Changchun Institute of Optics, Fine Mechanics and Physics (CIOMP), Chinese Academy of Sciences, 130033, P. R. China.
[c] State Key Laboratory of Physical Chemistry of Solid Surface, College of Chemistry and Chemical Engineering, Xiamen University, Xiamen 361005, China
[d] Collaborative Innovation Center of Chemistry for Energy Materials, Xiamen University, Xiamen 361005, China

Electronic Supplementary Information (ESI) available: [details of any supplementary information available should be included here]. See DOI: 10.1039/x0xx00000x

A hydrophobic MSNP could act as a burst microvalve in microchannels (Figure S1), the energy barrier which prevents fluid flowing is originated from the Laplace pressure (*ΔP*), which is described as[34]:

$$\Delta P = P_I - P_O = -\sigma(2\frac{\cos\theta_S}{W} + \frac{\cos\theta_S}{H-h} + \frac{\cos\theta_V}{H-h}) \quad (1)$$

where P_I and P_O are the pressures inside and outside the liquid, W are the widths of the microchannels, *H* is the height of the microchannels, *h* is the height of the MSNPs, σ is the surface tension of fluids, θ_S and θ_V are the advancing contact angles (ACAs) of fluids on the PDMS and MSNP surfaces, respectively. According to Equation (1), we figured out that the flow behaviour of fluids in microchannel could be manipulated by adjusting the dimensions of the MSNP. Following this principle, the UVS is fabricated by integrating a programmable silicon (Si) MSNP array with different lengths in a trapezoidal poly(dimethylsiloxane) (PDMS) microchannel. Through designing and calculating the relation position of the MSNPs, we divided the trapezoidal microchannel into 10 equal-volume chambers (Figure S2). The dimensions of the substrate structures and microchannels were controlled by adjusting the etching time of the fabrication process (Table S1, Figure S3 and Figure S4). The Si-MSNP array was modified by Trichloro(1H,1H,2H,2H-perfluorooctyl)silane (PFS), and θ_V and θ_S are 125.4±0.9° and 126.0±0.7°, respectively (Figure S5). Experimentally measured (P_{max}) and theoretical (*P*) burst pressures increase with the shortening of the length of the exposed MSNPs in microchannels (**Figure 1**m). We believe that the difference of pressure value between P_{max} and *P* is resulted from the pressure drop of water in the fluidic tube and the increased force area when water flows through new MSNPs. Therefore, we can stop the fluid front at desired MSNP by changing the applied pressure of the liquid inlet. For instance, when the applied pressures of liquid inlets were 89.0, 94.0. 97.0 and 104.0 mbar, water fronts stopped at the 2nd, 4th, 6th and 9th MSNP, respectively (Figure 1a-d). A gas inlet is designed to cut off the fluid column in the trapezoidal microchannel, and quantitative water liquid would be captured. As shown in Figure 1e-h, we changed the applied pressure of liquid and gas inlets to 0.0 and 100.0 mbar, respectively, measurable liquids were obtained. Feedback of the liquid volume is important information for a well-behaved syringe, and the volume can be calculated according to the floor space and the height of the liquid. However, the real curve shapes of TCL of the liquid ends are inconvenient to be observed and calculated, hence we fabricated narrow metering microchannel in the end of the UVS to reduce the measurement error. As shown in Figure 1i-l, we can continuously gain quantitative water liquids with different volumes (from 1.00 to 10.00 nL) by changing the applied pressure of the inlets with 98% accuracy (Figure 1n). The detailed process is shown in Video S1 Supporting Information.

Performance of the UVS

Larger and stable value of P_{max} could improve the accuracy rate of the dispensing process, hence the factors that influence the value of the P_{max} were discussed. First, MSNPs with different roughness were fabricated, and the microvalve functions were measured (**Table 1** and Figure S6). We found that the nanopillar structure could significantly improve the value and stability of $P_{max,}$ and the increase degree is proportional to the surface roughness, while excessive etching time of the nanopillar surface would decrease the θ_V and the manipulation ability for fluids. Then, MSNPs with same width but different heights and same height but different widths were fabricated. As shown in Table 1, P_{max} and *P* slightly get higher along with the increase of the MSNP height. We noted that higher MSNP possesses better stability for manipulating fluid in microchannels, hence we chose 1500 nm as the MSNP height in the following experiments. The results in Table 1 demonstrate that the MSNP width has no effect on the P_{max} and *P*. To reduce the volume error of the chambers, MSNP width of 10.0 μm was applied to fabricate the subsequent UVS.

The throughput of the UVS is an important parameter for the applicability of the device. The dispensing period includes two stages: water front stops at the edge of MSNP and gas cuts off liquid column. The duration of the first stage is related to the applied pressure of liquids, and high applied pressure increases the flow rate of fluids and decreases the flowing time (Figure S7a,b). As for the second stage, high gas pressure obviously corresponding to short dispensing duration (Figure S7c), while high cut-off speed of liquid column decreases the stability and increases the measuring error of the dispensing process (Figure S7d). The optimal applied pressures could be weighed between the accuracy and dispensing duration according to the requirements of its combined applications. The throughput of single UVS is undistinguished when compared to commercial Echo systems,[13-14] which could be make up by connecting the pressure pump to multiple UVSs.

The metering range of the UVS could be adjusted by altering the height of the microchannel (Figure S8**)**, and new correspondence relationships between liquid volume and manipulation pressure were established (Figure S9a,c,e). We also investigated the dispensing error of each UVS, as in Figure S9b,d,f. The minimum of the liquid volume that we can capture is 50 pL, and the accuracy is greater than 96% (Figure S10). The PDMS slab would collapse and block the UVS if we continue to reduce the dimensions of the microchannel.

Capture of sub-picoliter and femtoliter liquids by the glass-Si constructed UVS

Glass-Si constructed UVSs (G-UVS) were fabricated by standard anodic bonding method to lower the minimum volume of available liquid (Figure S11). There are two main factors that limit the magnitude of the minimum volume. The first is the resolution ratio of fabrication technology, which determines the dimension of microchannels. The minimum gap that we could precisely fabricate by etching technique is 1.5 μm in three dimensions. Second, successive dispensing of liquids with different volumes relies on enough difference among the P_{max} of MSNPs. Though the microchannel with lower dimension would increase the pressure difference (Figure S12i, Figure S13a, Figure S14g), the increased P_{max} of the MSNPs weaken the stability of the dispensing process and reduces the accuracy of the device, simultaneously. Therefore, the length difference among the MSNPs should be increased as much as possible. In addition, there should be certain spacing among the MSNPs to reduce the error caused by the MSNPs volume. Based on the factors, four kinds of G-UVSs with different quantities of chambers were prepared (Table S1). The minimum volume of the G-

UVS with ten chambers (10-G-UVS) could dispense is 6.0 pL (Figure S12a-h), and the accuracy rate is larger than 97% (Figure S12j). The 5-G-UVS could capture 1.5 pL liquids with 96% accuracy (Figure 2 and Figure S13). As for the 3-G-UVS, the minimum is 0.5 pL with 96% accuracy (Figure S14). Due to the lack of the limit of above-mentioned pressure differences among the MSNPs, the available volume of the 1-G-UVS is far lower compared to the above devices, which is 25 fL with 97% accuracy (Figure S15a-d). The liquid volume could be adjusted by changing the distance between the MSNPs and the intersection of the microchannels (Figure 15e).

Dispensing wide surface tension ranges and multiphase liquids

To demonstrate the applicability of the UVS for multipurpose microfluidics system, it is necessary to investigate its manipulation ability for multiple kinds of liquids. PFS-blended PDMS microchannels were used to enhance the hydrophobicity and control performance of the devices in this section,[35] and the θ_S can reach 130.5±0.7°. As shown in **Figure 3**a-d and Figure S16a-d, quantitative ethanol aqueous solution (from 5% to 30%) could be obtained by the UVS (Figure S17, Video S2 Supporting Information). In addition, measurable multiphase liquids including rapeseed oil, bovine blood, Bull serum albumin (BSA) and insulin solutions (Figure 3e-l), and the applicable dispensing pressure of the UVS could be adjusted according to the ST of the liquid. When the ST of the solution (40% alcohol) decreases to 28.2 mN/m (Figure S16e,f), the manipulation ability for TCL on the MSNPs start to be unstable, and the differences of P_{max} among the MSNPs are too small to stop the fluid front in desired position. There is even leakage in the gas inlet when the ST of the fluid drops to 25.5 mN/m, indicating the UVS is no longer suitable (Figure S16g,h).

Quantitative mixing of liquids in microchannels

Quantitative micromixing devices were fabricated by integrating two UVSs together in a chip (**Figure 4**a). 10 times in increments of 1.0 nL fluorochrome liquids could be dispensed by the two UVSs, then the liquid successively flowed into the serpentine mixing microchannel and the detection chamber. Six gradient proportions of the fluorochrome solutions were obtained (Figure 4b-n), which means that the device could be utilized to simultaneously dispense multiple kinds of gradient concentration solutions in microfluidics.

Integrated microchip for preparing morphologically controllable metal nanocrystals

Besides preparing quantitative gradient concentration solutions, the UVS could be used to precisely control the reagent dosage in trace-volume chemistry reactions, which provides new opportunities in resource-limited settings, measurable cell cultures, single-cell drug injection, and lab-on-chip applications.[10-11] As an example, an integrated microchip embedded with three UVSs was fabricated (**Figure 5**a). Gradient-size gold nanoparticles were prepared following the well-established literature method in the device.[36] First, 8.00 nL (desired volume, same below) gold(III) chloride solution was dispensed by UVS-1 to mix with 2.00 nL PVP solution captured by UVS-2 in the first blend microchannel. Then 2.00, 4.00 and 6.00 nL ascorbic acid solutions were captured by the UVS-3, respectively, and mixed with the above-mentioned solution in the second blend microchannel (Figure S18). Figure 5b-d shows the TEM images of the gradient Au nanoparticles, and the diameter of the Au nanoparticle increases along with the decrease of the ascorbic acid solution volume (Figure S19). To prove the applicability of the strategy, the Au nanorods with anisotropic shapes were synthesized using the seed-growth method (Figure S20).[37] As shown in Figure 5e-g, the aspect ratio of the Au nanorods could be controlled by changing the addition amount of Ag^+ (Figure S21).[38] As for complicated microfluidic synthesis system and lab-on-chip platforms, the relative position and quantity of the UVS could be designed according to the demand of the synthetic method, and the product of each reaction step in the microchip could be immediately used for characterizing without secondary sample preparation.

Conclusions

In conclusion, pressure-controlled UVS are prepared to dispense quantitative sub-picoliter liquid in microfluidics. The liquid volume could be changed by adjusting the applied pressure of the inlets and the dimensions of the microchannels. To further improve the microvalve stability of the UVS and maximally decrease the dispensing error of the liquid, nanopillar embedded microstripe array is fabricated and adopted as the substrate of the UVS. Simultaneously, feedback microchannel for measuring the liquid volume is integrated in the device, and the accuracy of the UVS could reach 96%. Furthermore, G-UVS is proposed to reduce the volume of available liquid, which could dispense ultramicro-volume liquids in increments as low as 0.5 pL. Single femtoliter liquid was also successfully dispensed with 97% accuracy in the G-UVS. The UVS also exhibits strong ability for capturing quantitative wide ST ranges and multiphase liquids, which demonstrates its applicability for common microfluidics system. Practical synthesis system in bulk reaction was conducted in a lab-on-chip platform with three UVSs, and controllable synthesis of gradient-size and anisotropic metal nanocrystals were produced by adjusting the volume of reaction reagent. A collecting device is connected to the microchip, and the product of the quantitative reaction by the UVS could be directly collected and used for characterization. As for intricate lab-on-chip synthesis system, the quantity, measuring range and relative location of the UVS could be freely designed according to requirements, and we anticipate that the principle of the UVS will be beneficial in the fields ranging from the researches for lab-on-chip platforms, analytical chemistry for medicine to quantitative cell cultures, even drug injection for single cell and beyond.

Author contributions

N.Y., Y.L. and J.Z. designed the study; N.Y. S.W. and X.T. performed the experiments; P.G., J.N. and B.Y. carried out the data analysis; J.Z. wrote the paper with help from all authors.

Conflicts of interest

The authors declare no conflicts.

Acknowledgements

This work was supported by the National Natural Science Foundation of China (Grant no. 21474037, 21774043 and

61727813), this project was also supported by the State Key Laboratory of applied optics and Doctor Interdisciplinary Research Funding Scheme of Jilin University.

Notes and references

1 C. D. Chin, V. Linder, S. K. Sia, *Lab Chip* 2012, **12**, 2118-2134.
2 O. Tokel, F. Inci, U. Demirci, *Chem. Rev.* 2014, **114**, 5728-5752.
3 R. Karnik, F. Gu, P. Basto, C. Cannizzaro, L. Dean, W. Kyei-Manu, R. Langer, O. C. Farokhzad, *Nano. Lett.* 2008, **8**, 2906-2912.
4 S. G. Van Ornum, R. M. Champeau, R. Pariza, *Chem. Rev.* 2006, *106*, 2990-3001.
5 C. A. Stewart, Y. Finer, B. D. Hatton, *Sci. Rep.* 2018, **8**, 895-893.
6 W. Gu, X. Y. Zhu, N. Futai, B. S. Cho, S. Takayama, *Proc. Natl Acad. Sci.USA* 2004, **101**, 15861-15866.
7 A. J. Leite, M. B. Oliveira, S. G. Caridade, J. F. Mano, *Adv. Funct. Mater.* 2017, **27**, 1701219.
8 A. A. Popova, D. Marcato, R. Peravali, I. Wehl, U. Schepers, P. A. Levkin, *Adv. Funct. Mater.* 2018, **28**, 1703486.
9 X. Liu, L. Chen, H. Liu, G. Yang, P. Zhang, D. Han, S. Wang, L. Jiang, *NPG Asia Mater.* 2013,**5**,e63-e72.
10 F. De Angelis, M. Malerba, M. Patrini, E. Miele, G. Das, A. Toma, R. P. Zaccaria, E. Di Fabrizio, *Nano. Lett.* 2013, **13**, 3553-3558.
11 R. Elnathan, B. Delalat, D. Brodoceanu, H. Alhmoud, F. J. Harding, K. Buehler, A. Nelson, L. Isa, T. Kraus, N. H. Voelcker, *Adv. Funct. Mater.* 2015, **25**, 7215-7225.
12 Y.-C. Wu, T.-H. Wu, D. L. Clemens, B.-Y. Lee, X. Wen, M. A. Horwitz, M. A. Teitell, P.-Y. Chiou, *Nat. Methods* 2015, **12**, 439-444.
13 Men, Y. Fu, Z. Chen, P. A. Sims, W. J. Greenleaf, Y. Huang, *Anal. Chem.* 2012, **84**, 4262-4266.
14 K. Honarnejad, A. Daschner, A. Giese, A. Zall, B. Schmidt,A. Szybinska, J. Kuznicki and J. Herms, PLoS One,2013, 8(11), e80645.
15 R. Garcia, A. W. Knoll, E. Riedo, *Nat. Nanotech.* 2014, **9**, 577-587.
16 J. Pablo Agusil, N. Torras, M. Duch, J. Esteve, L. Perez-Garcia, J. Samitier, J. A. Plaza, *Adv. Funct. Mater.* 2017, **27**, 1605912.
17 G. M. Whitesides, *Nature* 2006, **442**, 368373.
18 E. K. Sackmann, A. L. Fulton, D. J. Beebe, *Nature* 2014, **507**, 181-189.
19 K. S. Elvira, X. C. i. Solvas, R. C. R. Wootton, A. J. deMello, *Nat. Chem.* 2013, **5**, 905-915.
20 L. Jiang, Y. Lu, Z. P. Dai, M. H. Xie, B. C. Lin, *Lab Chip* 2005, **5**, 930-934.
21 C. T. Culbertson, T. G. Mickleburgh, S. A. Stewart-James, K. A. Sellens, M. Pressnall, *Anal. Chem.* 2014, **86**, 95-118.
22 J.-A. Lv, Y. Liu, J. Wei, E. Chen, L. Qin, Y. Yu, *Nature* 2016, **537**, 179-184.
23 M. T. Guo, A. Rotem, J. A. Heyman, D. A. Weitz, *Lab Chip* 2012, **12**, 2146-2155.
24 H.-H. Jeong, B. Lee, S. H. Jin, S.-G. Jeong, C.-S. Lee, *Lab Chip* 2016, **16**, 1698-1707.
25 T. Gu, C. Zheng, F. He, Y. Zhang, S. A. Khan, T. A. Hatton, *Lab Chip* 2018, **18**, 1330-1340.
26 O. Guillaume-Gentil, E. Potthoff, D. Ossola, C. M. Franz, T. Zambelli, J. A. Vorholt, *Trends Biotechnol.* 2014, **32**, 381-392.
27 O. Guillaume-Gentil, R. V. Grindberg, R. Kooger, L. Dorwling-Carter, V. Martinez, D. Ossola, M. Pilhofer, T. Zambelli, J. A. Vorholt, *Cell* 2016, **166**, 506-516.
28 K. W. Oh, C. H. Ahn, *J. Micromech. Microeng* 2006, **16**, R13-R39.
29 P. N. Nge, C. I. Rogers, A. T. Woolley, *Chem. Rev.* 2013, **113**, 2550-2583.
30 A. Puntambekar, J. W. Choi, C. H. Ahn, S. Kim, V. Makhijani, *Lab Chip* 2002, **2**, 213-218.
31 A. Mepham, J. D. Besant, A. W. Weinstein, I. B. Burgess, E. H. Sargent, S. O. Kelley, *Lab Chip* 2017, **17**, 1505-1514.
32 G. Takei, M. Nonogi, A. Hibara, T. Kitamori, H.-B. Kim, *Lab Chip* 2007, **7**, 596-602.
33 Y. Ouyang, S. Wang, J. Li, P. S. Riehl, M. Begley, J. P. Landers, *Lab Chip* 2013, **13**, 1762-1771.
34 N. Yu, S. Wang, H. Liu, P. Ge, J. Nan, S. Ye, J. Zhang, B. Yang, *Sens. Actuators, B* 2018, **256**, 735-743.
35 J. Zhang, B. Yang, *Adv. Funct. Mater.* 2010, **20**, 3411-3424.
36 J. Wagner, J. M. Kohler, *Nano. Lett.* 2005, **5**, 685-691.
37 M. Liu, P. Guyot-Sionnest, J. Phys. Chem. B 2005, **109**, 22192–22200.
38 T. K. Sau, C. J. Murphy, J. Am. Chem. Soc. 2004, **126**, 8648–8649.

View Article Online
DOI: 10.1039/C9LC00730J

COMMUNICATION

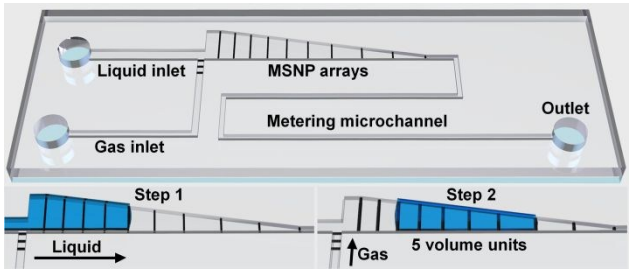

Scheme 1. Schematic illustration of the capture process of quantitative liquids by the UVS.

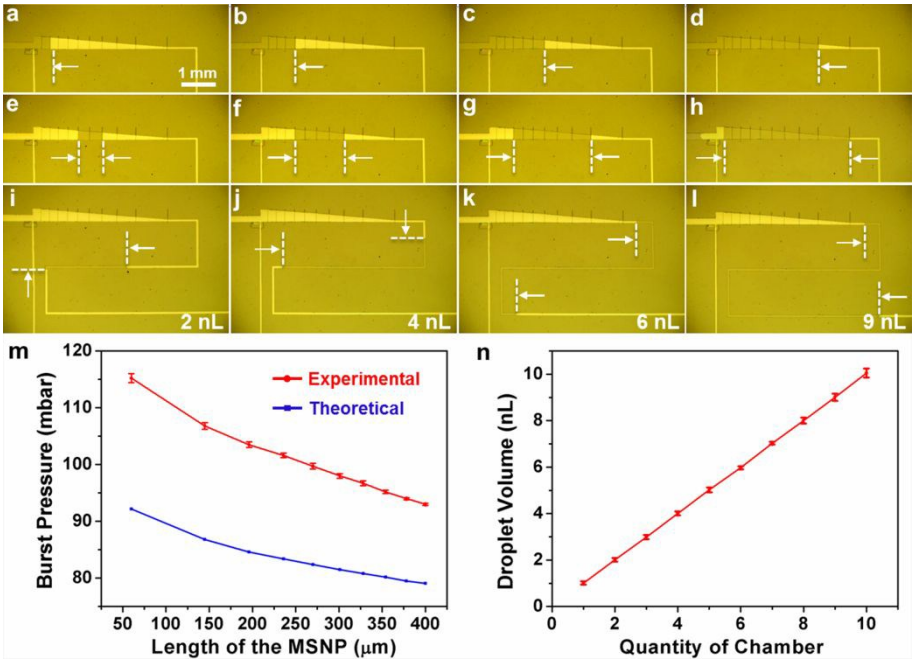

Figure 1. (a-d) Optical microscopy images of the dispensing process of water in the UVS. When the applied pressures of liquid inlets are 89.0, 94.0, 97.0 and 106.0 mbar, water front stop at the 2nd (a), 4th (b), 6th (c) and 9th (d) MSNP, respectively. The positions of white arrows represent the ends of the liquids. The height of the microchannel is 10.0 μm. The volume of each chamber is 1.00 nL theoretically. (e-h) 0.0 mbar of liquid inlets and 100.0 mbar of gas inlets are applied to capture quantitative liquids in the UVS. The volumes of the water liquids are 1.97 (i), 3.91 (j), 5.97 (k), 8.99 nL (l), respectively. The figures in the images represent the desired liquid volumes. (m) Experimentally measured and theoretical bursting pressures as a function of the length of exposed MSNPs in the microchannels. (n) Repeatability of the UVS. The measured water volume dispensed as a function of chamber quantity. Errors bars represent standard error.

View Article Online
DOI: 10.1039/C9LC00730J

Table 1. The *P* and P_{max} upon different dimensions of the MSNPs.

MSNP	Height [nm]	Width [μm]	Roughness of nanopillar surface [Rq·nm]	ACA of nanopillar surface [°]	*P* [mbar]	P_{max} [mbar]
Microstripes	1500±18	10.0±0.09	0.142±0.114	112.4±2.1°	74.3±2.8	91.1±4.6
1	1500±18	10.0±0.09	1.658±0.198	118.4±0.5°	77.5±0.8	94.3±0.4
2	1500±18	10.0±0.09	4.092 ±0.253	120.4±1.2°	78.9±1.4	96.4±0.7
3	1500±18	10.0±0.09	8.859 ±0.376	121.4±1.0°	80.3±1.1	96.9±0.6
4	1500±18	10.0±0.09	12.246±0.738	125.4±0.9°	83.1±1.0	98.0±0.7
5	1500±18	10.0±0.09	10.316±0.791	123.4±1.2°	81.8±1.5	95.3±0.4
6	320±4	10.0±0.09	12.672±0.642	125.2±0.8°	77.5±0.9	96.6±1.2
7	630±9	10.0±0.09	13.457±0.814	125.6±0.6°	79.2±0.7	96.9±0.9
8	1000±12	10.0±0.09	12.361±0.569	124.9±1.4°	80.7±1.6	97.3±0.6
9	1300±14	10.0±0.09	12.548±0.672	124.8±1.3°	82.0±1.5	97.5±0.8
10	1500±18	20.0±0.12	12.583±0.832	124.6±1.5°	82.6±1.7	98.2±0.2
11	1500±18	30.0±0.18	13.141±0.948	125.8±0.7°	83.5±0.9	98.7±0.6
12	1500±18	40.0±0.22	12.763±0.835	124.1±0.4°	82.2±0.5	97.6±0.9

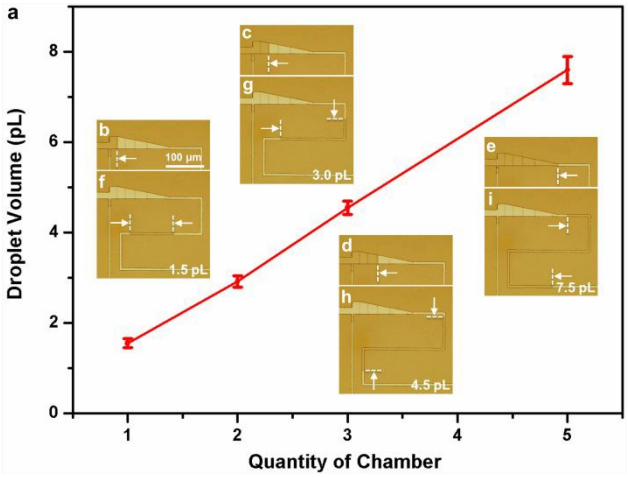

Figure 2. (a) The measured water volume dispensed as a function of chamber quantity. Errors bars represent standard error. (b-i) Optical microscopy images of the 5-G-UVS which could capture picoliter liquids. 278.0, 297.0, 315.0 and 449.0 mbar of the liquid inlet pressures are applied to stop the water front on the 1st (b), 2nd (c), 3rd (d) and 5th (e) MSNP, respectively. 500.0 mbar of the gas inlets are applied to capture 1.48 (f), 2.92 (g), 4.54 (h) and 7.51 pL (i) water liquids, respectively. The figures in the images represent the desired liquid volumes.

View Article Online
DOI: 10.1039/C9LC00730J

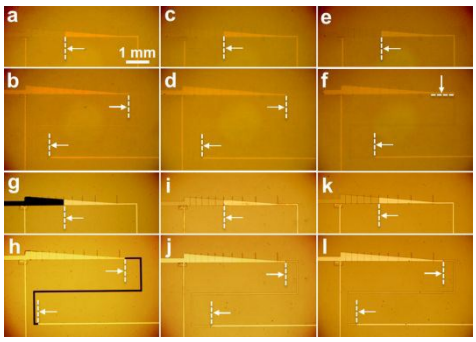

Figure 3. (a-l) Optical microscopy images of the UVS for capturing wide ST ranges and multiple kinds of liquids. The height of the microchannel is 10.0 µm, and the desired liquid volume is 6.00 nL. (a,b) 5% alcohol, ST is 57.4 mN/m, the manipulation pressures of liquid and gas inlets are 95.0 and 94.0 mbar, respectively. (c,d) 30% alcohol, ST is 37.1 mN/m, the manipulation pressures of liquid and gas inlets are 55.0 and 80.0 mbar, respectively. (e,f) Rapeseed oil, ST is 31.6 mN/m, the manipulation pressures of liquid and gas inlets are 35.0 and 100.0 mbar, respectively. (g,h) Bovine blood, ST is 72.5 mN/m, the manipulation pressures of liquid and gas inlets are 99.0 and 150.0 mbar, respectively. (i,j) BSA (25 mg/mL), ST is 52.5 mN/m, the manipulation pressure of liquid and gas inlets are 89.0 and 90.0 mbar, respectively. (K,l) Insulin (100 mg/L in HCL, PH=2), ST is 72.1 mN/m, the manipulation pressure of liquid and gas inlets are 98.0 and 100.0 mbar, respectively.

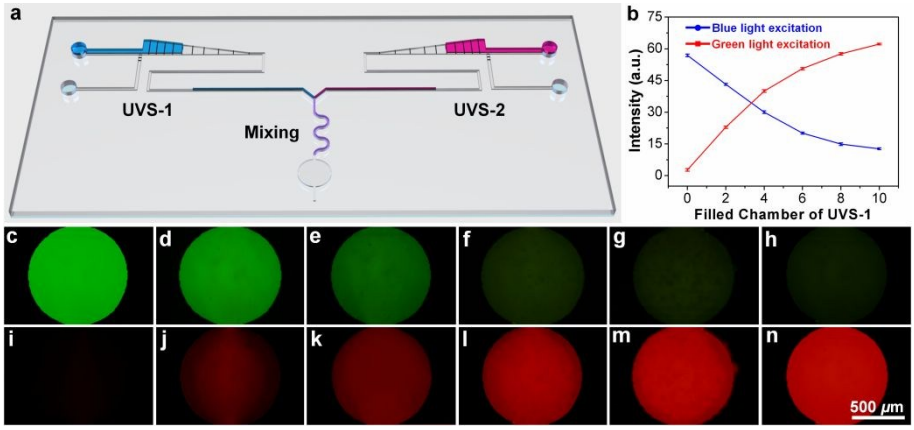

Figure 4. (a) Schematic of the UVS for mixing quantitative liquids. The end of the serpentine mixing microchannel is connected to the outlets of the two UVS and a detection chamber, and the diameter of the fluorescent detection chamber is 1000.0 μm. The height of the microchannel is 10.0 μm. (b) The fluorescence intensity of the detection chamber under blue and green light excited fluorescent microscopy. Errors bars represent standard error. The fluorescent microscopy images of the mixed dyes under blue (c-h) and green (i-n) light excited fluorescent microscopy. The desired liquids volumes of the sodium fluorescein and rhodamine solutions are 10.0 and 0.0 nL (b,i), 8.0 and 2.0 nL (c,j), 6.0 and 4.0 nL (d,k), 4.0 and 6.0 nL (f,l), 2.0 and 8.0 nL (g,m), 0.0 and 10.0 nL (h,n), respectively.

View Article Online
DOI: 10.1039/C9LC00730J

COMMUNICATION

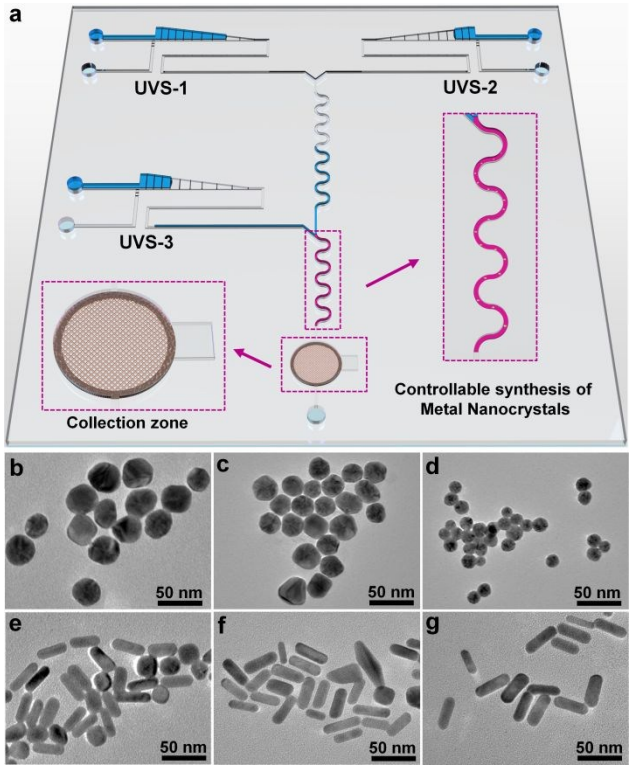

Figure 5. (a) Schematic of the integrated UVS for producing gradient-size and anisotropic Au nanocrystals. (b-d) The TEM images of the gradient-size Au nanoparticles. The liquid volumes of the gold(III) chloride solution and PVP solution are identical in each experiment. The liquid volumes of the ascorbic acid solution are 2.02 (b), 4.12 (c) and 6.00 (d) nL, respectively. (e-g) The TEM images of the Au nanorods with anisotropic shapes. The liquid volumes of the ascorbic acid solution in the UVS-2 and the Au seed solution in the UVS-3 are identical in each experiment. The liquid volumes of the premixed solutions ($Au^{[3+]}$, $Ag^{[+]}$, and CTAB solution) are 3.07 (b), 4.92 (c) and 7.05 (d) nL, respectively.